

Featured Articles

Combustion Analysis Techniques for Development of Next-generation Engine Systems

Yoshihiro Sukegawa
Kazuhiro Oryoji
Eiji Ishii, Dr. Eng.

OVERVIEW: Improving the fuel economy and emissions of vehicle engines requires a detailed understanding of the various physical processes taking place inside the engine so as to identify optimal combustion control techniques and engine component designs. Based on numerical techniques established by its power plant business for the analysis of two-phase flow, combustion, and other phenomena, Hitachi has developed techniques for using simulations to estimate flow, mixture formation, and combustion in engine cylinders. Hitachi has also combined these estimation techniques with a concentration physical simulation model for PM such as soot, an area in which there has been strong demand for emission reductions in recent years. This model calculates the process of PM formation based on detailed chemical reaction mechanisms. Hitachi has gone on to use this new combustion simulation technique to propose a combustion control concept that reduces emissions at cold engine start-up.

INTRODUCTION

PROVIDING vehicle engines with cleaner exhaust gas and better fuel economy is important for making effective use of energy resources and protecting the environment. The development of engine control techniques and components capable of efficient combustion are essential to overcoming these challenges.

For example, the fuel economy and emissions of direct injection gasoline engines (a type of fuel-efficient engine that is becoming increasingly common) are improved through the precise control of fuel spray, air flow, and other processes inside the cylinder to achieve a suitable mixture for combustion. This involves optimizing a wide variety of parameters, including the fuel spray and gas flow, injection, ignition, and valve timing. Using computer simulations to analyze the behavior of the fuel, air, and combustion gas in detail is an effective technique for efficiently identifying the optimal combination of these parameters.

Engines are characterized by the presence of complex dynamic phenomena such as those associated with the mutual interaction of gases and liquids, chemical reactions, turbulent flow, and moving boundaries. To deal with these accurately, Hitachi uses

engine analysis techniques that were developed by making enhancements to numerical analysis techniques established by Hitachi's power plant business for two-phase flow, combustion, and other phenomena.

This article describes the computational methods used in simulation techniques for estimating engine flow, combustion, and exhaust, and presents examples of their use for engine analysis.

USE OF COMPUTER SIMULATIONS FOR COMBUSTION ANALYSIS

In the case of a direct injection gasoline engine, the following phenomena occur within each engine stroke.

- (1) The down-stroke of the piston draws in air (gas flow).
- (2) Fuel is injected into the air inside the cylinder.
- (3) A fuel-air mixture is formed by fuel vaporization from the injected fuel droplets and air.
- (4) Ignition causes flame propagation in the mixture, resulting in a rise in the temperature and pressure inside the cylinder.
- (5) The nitrogen oxides (NO_x), particulate matter (PM), and other compounds formed during combustion become the emissions.

Accordingly, a combustion simulation needs to model the gas flow, fuel spray behavior, droplet

vaporization, mixing of air and fuel, flame propagation, formation of emissions, and other phenomena, and to obtain these numerically. The following sections describe the mathematical models used for the main phenomena, as well as the computational methods used.

Gas Flow and Fuel Spray Model

The flow and mixing of gas is obtained by solving the equations for the conservation of mass, momentum, and energy in the mixture, and for the conservation of mass of the fuel components and combustion gas. These conservation equations are represented by the following partial differential equation (equation 1).

$$\frac{\partial F}{\partial t} + \frac{\partial V_i F}{\partial x_i} + \frac{\partial q_i}{\partial x_i} + S = 0 \quad (1)$$

Where, t represents time, x_i represents the coordinates, and V_i represents the gas velocity ($i=1, 2, 3$). The first term on the left represents the variation with time, the second term represents the convection, the third term represents diffusion due to molecular motion and turbulent flow, and the fourth term represents the creation or elimination of physical quantity (“source term”). F is a vector comprising the physical values to be solved for, which include the mixture density, momentum, internal energy, fuel component density, and combustion gas density. The q_i term represents phenomena that come about due to the spatial gradient of physical quantities, such as the stress due to viscosity and the flux due to conduction and diffusion. For example, equation (2) is a conservation of momentum equation that represents the stress resulting from molecular viscosity and eddy viscosity.

$$q_i = (\mu_m + \mu_t) \frac{\partial V_i}{\partial x_i} \quad (2)$$

Where, μ_m is the coefficient of molecular viscosity and μ_t is the coefficient of eddy viscosity. The coefficient of eddy viscosity is obtained using turbulence models. Turbulence models can be broadly divided into Reynolds-averaged Navier-Stokes simulation (RANS) time-averaged turbulence models and large eddy simulation (LES) space-averaged turbulence models. Since LES can perform more detailed analyses than RANS, being able to deal directly with transient turbulent flow behavior, the method described here uses LES.

The conservation equations are coupled with the gas state equation to obtain the gas pressure and temperature.

$$P = \rho T \sum Y_j R_j \quad (3)$$

Where, Y_j is the mass fraction of component j and R_j is the gas constant for component j . The finite volume method⁽¹⁾ is used for the spatial discretization of equation (1). The finite volume method splits the flow field into computational cells consisting of small polygons (see Fig. 1) and formulates the balance of flux across the cell boundaries and the quantities created or eliminated within the cell as shown in equation (4).

$$\frac{d}{dt} (\Delta V_k \cdot F_k) = -\sum_i V_{Ci} F_i \cdot \Delta S_i - \sum_i q_i \cdot \Delta S_i + \Delta V_k \cdot S_k \quad (4)$$

Since equation (4) is an ordinary differential equation with respect to time, numerical integration methods such as the Euler or Runge-Kutta methods can be used to solve it for each time step.

The fuel spray behavior is obtained using a discrete droplet model (DDM)⁽²⁾ which introduces particles representing droplets into the gas flow field and tracks their movements. Because the actual number of droplets in the engine is very large, modeling them all in a computer is impractical. Instead, the method tracks the behavior of a group of particles, called a “parcel,” that comprises a number of droplets with the same initial conditions (size, velocity, temperature, and coordinates) (see Fig. 2). Equation (5) is the equation for the motion of a parcel.

$$\frac{dV_d}{dt} = -\frac{3\rho}{4\rho_d d} C_D |V - V_d| (V - V_d) \quad (5)$$

Where, V_d is the parcel velocity, V is the gas velocity, C_D is the drag coefficient, ρ_d is the droplet density, and d is the droplet diameter. The instantaneous velocity of a parcel can be obtained from equation (5), and the

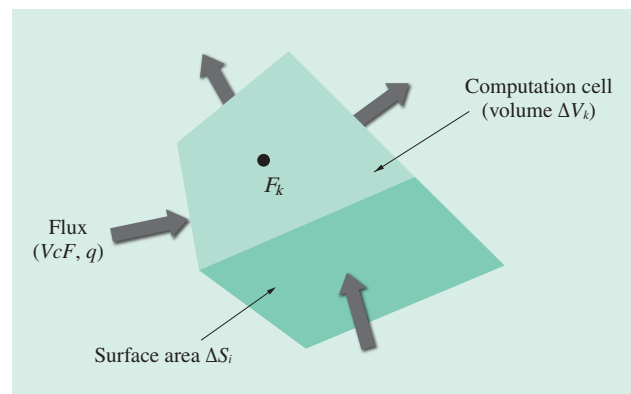


Fig. 1—Computation Cell for Finite Volume Method. The figure shows the computation cell for the finite volume method and the model diagram of the flux across the cell surface.

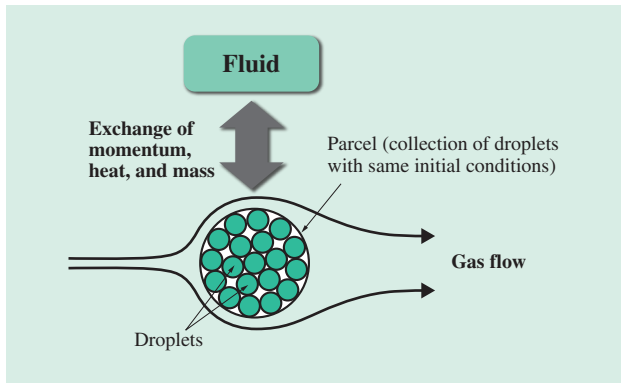


Fig. 2—Use of Parcels to Model Droplets.

The diagram shows the concept behind using parcels to model droplets. The droplets are modeled as parcels, each of which is made up of a number of droplets treated as having the same initial conditions.

trajectory of the parcel at any point can be determined by integrating this velocity over time.

An exchange of momentum occurs between droplet and gas via friction, an exchange of heat via heat transfer, and an exchange of mass via evaporation. These processes are represented on the gas side by the source term in equation (1).

When a DDM is used for the analysis of engine combustion, a number of sub-models are adopted in addition to the parcel's conservation of energy equation to consider factors such as evaporation, breakup, drag, collisions with walls, and turbulence.

To take account of the injection of fuel into the engine, the DDM requires that the physical quantities (coordinates, velocity, diameter) of a parcel at a fuel injector be provided as boundary conditions. These are obtained by a spray formation simulation⁽³⁾ that performs an integrated analysis of the liquid flow, liquid film formation, and process by which the film breaks up into droplets in the fuel injector nozzle (see Fig. 3). This simulation uses the particle method (a mesh-free method for the micro-level tracking of the gas-liquid interface), which can model atomization from the injectors with comparatively low computational requirements.

Combustion Model

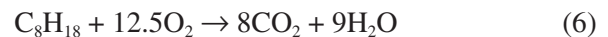
Combustion is a chemical reaction between fuel and oxidizer. The temperature, pressure, and other changes that result from combustion are calculated as the consequence of changes in the gas composition resulting from the reaction.

The combustion of gasoline can be approximated by the overall reaction shown in equation (6).



Fig. 3—Simulation of Spray Formation by Injector.

This shows an example of using the particle method to simulate the behavior of fuel sprayed from the nozzle of a swirl-type fuel injector. The simulation involves an integrated analysis that considers the formation of a liquid film in the nozzle and the formation of droplets by the breakup of the film.



By introducing the progress variable C ($= 0-1$), which represents the progress of the reaction from the left side of the equation to the right, the gas composition can be obtained using this progress variable and the fraction of the fuel component f . For example, the mass fractions of the fuel (C_8H_{18}) and oxygen (O_2) are given by equation (7) in the case when fuel and air combust in accordance with the stoichiometric mixture ratio.

$$\left. \begin{aligned} Y_{\text{C}_8\text{H}_{18}} &= f(1-C) \\ Y_{\text{O}_2} &= 0.233(1-f)(1-C) \end{aligned} \right\} \quad (7)$$

Since multiplying the progress variable C by the mixture density ρ gives the burned gas density, the progress variable can be obtained by solving the conservation of mass equation for the burned gas in the form of equation (1).

The rate at which combustion progresses is determined by the source term in the conservation of mass equation for the burned gas, and how to express this source term is the key to combustion modeling. Under the conditions in an engine cylinder, the strength of the flow varies widely depending on driving conditions and spatial position. Accordingly, what is needed is a combustion model with a wide scope of application regardless of the flow conditions. A hyperbolic tangent approximation (HTA) combustion model⁽⁴⁾ was selected to satisfy this criterion. While the progress variable C progresses from 0 to 1 in the flame zone, there is likely to be a degree of consistency in

the shape of the C distribution. Accordingly, the HTA model uses equation (8) to represent this distribution.

$$C = \frac{1}{2} \left[1 + \tanh \left[\frac{2x}{\delta} \right] \right] \quad (8)$$

Where, δ is the flame thickness and x is the distance in the thickness direction. Considering the one-dimensional conservation of mass equation for the burned gas and assuming the C distribution is approximated by equation (8), equation (9) is obtained by solving for the rate of creation of burned gas ω .

$$\omega = \frac{8\rho_u S_L C^2 (1-C)}{\delta} \quad (9)$$

This model can be used for both laminar and turbulent flow cases. Furthermore, because it is independent of the turbulent flow model, the model has a wide range of applications including use with RANS or LES.

Emission Model

The emissions resulting from engine combustion, which need to be estimated, consist primarily of NO_x, unburned hydrocarbons (HC), carbon monoxide (CO), and PM. The following section describes the model used to calculate PM emissions.

PM is the result of particles formed by processes such as volatile fuel components condensing or reacting chemically. Regulations on PM are becoming stricter throughout the world, with strong demand for vehicle engines to achieve combustion with low PM emissions.

Fig. 4 shows the process of PM formation and growth. Formation and growth can be broadly divided into two stages. First, a gas-phase reaction forms PM precursors. This is then followed by a solid-phase reaction causing the PM formed by the collision of precursors to grow in size. Starting from the acetylene formed by the thermal decomposition of hydrocarbon fuel, the gas-phase reaction forms benzene and also polycyclic aromatic hydrocarbons (PAHs) made up of multiple benzene rings linked together. These PAHs are the precursors of PM. The formation and growth of PM take place in the solid-phase reaction, which consists of the formation of PM through collisions between PAHs (nucleation), collisions between PM and PAHs or acetylene (surface reactions), and collisions between PM (condensation).

A two-equation model is used for the solid-phase reaction⁽⁵⁾. This model estimates the PM number density and mass by solving for their variation over time. It is assumed that the variation over time

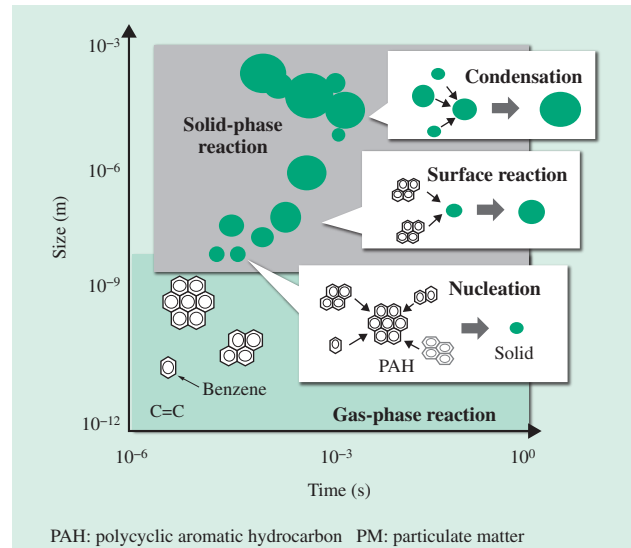


Fig. 4—PM Formation and Growth Process.

The graph shows the formation and growth of PM, with the horizontal axis representing the elapsed time and the vertical axis representing the particle size.

in the number density depends on nucleation and condensation, and that the variation over time in the mass depends on nucleation and surface reactions. For example, equation (10) represents the rate of formation of PM particles in terms of their number density [the particulate number (PN)].

$$\frac{d(\text{PN})}{dt} = R + W - G \quad (10)$$

Where, R is the nucleation rate, W is the surface reaction rate, and G is the condensation rate, each of which needs to be modeled. For example, the model represented by equation (11), which assumes acetylene as the PM precursor, is proposed for the nucleation rate⁽⁶⁾.

$$R = c_1 N_A \left[\frac{\rho Y_{\text{C}_2\text{H}_2}}{M_{\text{C}_2\text{H}_2}} \right] \exp \left[-\frac{21100}{T} \right] \quad (11)$$

Where, N_A is Avogadro's number, $Y_{\text{C}_2\text{H}_2}$ is the acetylene concentration, $M_{\text{C}_2\text{H}_2}$ is the molecular weight of acetylene, T is the temperature, and c_1 is a model constant. Since the acetylene and other components present in trace quantities are not considered in the overall equation [equation (6)], solving the PM model equation requires the use of elemental reaction equations (chemical reaction formulae for smallest units) to calculate the chemical reactions in detail. In this study, the components present in trace quantities are obtained by solving the elemental reaction equations for 781 chemical species and 2,247 reaction

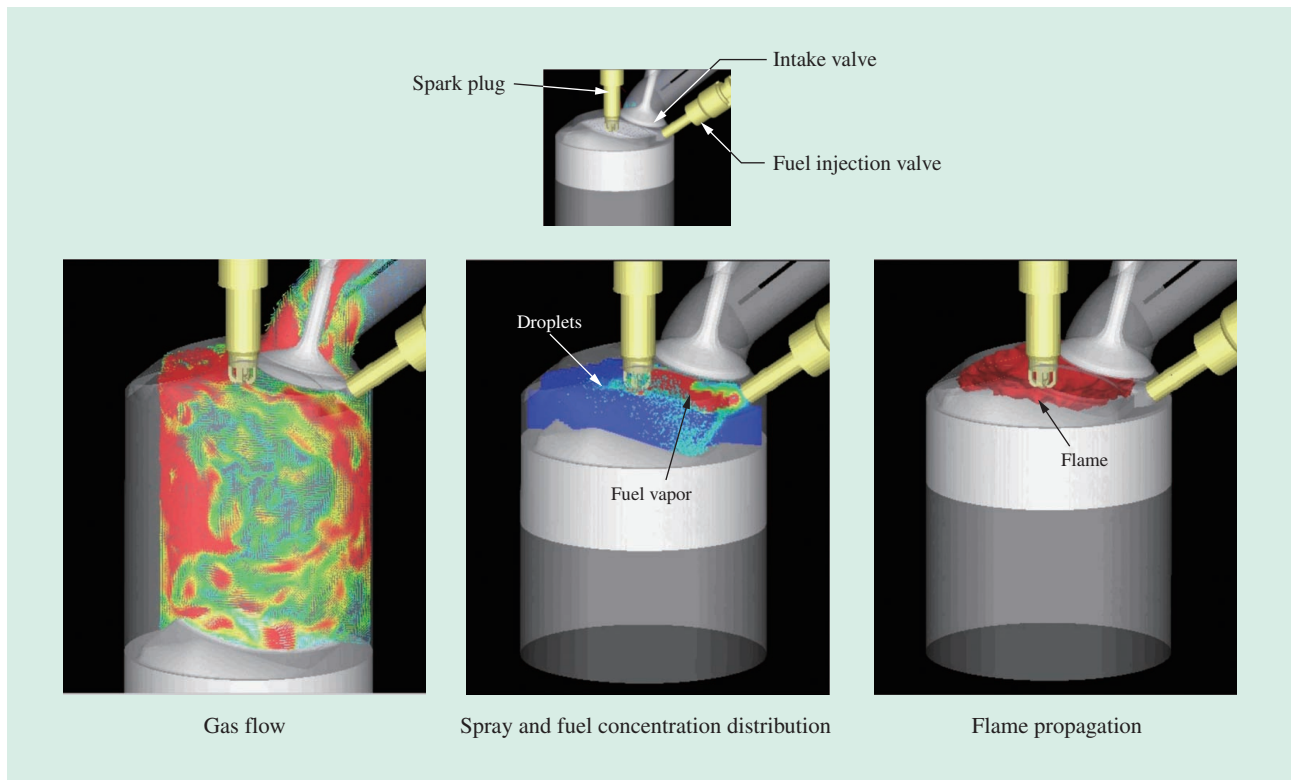


Fig. 5—Example Application of Combustion Simulations to Direct Injection Gasoline Engine.

The figures show a simulation of a direct injection gasoline engine. On the left is a vector diagram of air velocity for a vertical cross-section through the center of the intake valve. The vector color represents the magnitude of the velocity, with red being fastest. The center figure shows the spray droplet distribution and fuel concentration distribution for a vertical cross-section through the center of the cylinder. The color represents the fuel concentration, with red being highest. The right-hand figure shows a three-dimensional representation of the flame surface shape.

formulae for gasoline combustion, based on isoctane and normal heptane being the main fuel components.

By utilizing the computational methods described above, it is possible to perform a coupled simulation that extends from the engine intake stroke to the exhaust stroke and encompasses gas flow, fuel-air mixture formation, flame propagation, and emissions formation. Fig. 5 shows the use of the method to simulate a direct injection gasoline engine.

EXPERIMENTAL VERIFICATION OF SIMULATIONS

Verification of Gas Flow and Spray Simulations

Fig. 6 shows a comparison of experimental measurements and simulation results⁽⁷⁾ for the flow in an engine cylinder. The results indicate that the simulation can reproduce the flow with good accuracy, including good agreement for the pattern and velocity of the circulating flow that occurs at the bottom of the intake valve.

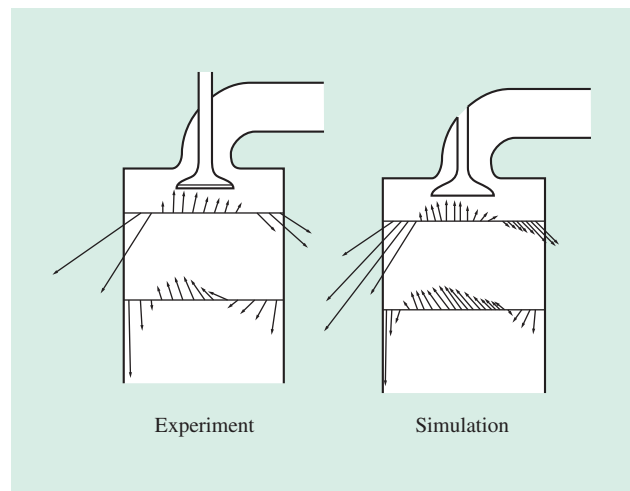


Fig. 6—Comparison of Simulation Results and Experimental Measurements for Flow in Engine Cylinder.

The diagrams show the air velocity vector in an engine cylinder. The vector length represents the magnitude of the velocity. The diagram on the left shows the measurement results from a laser Doppler flowmeter, and the diagram on the right shows the simulation results. A circulating flow occurs under the intake valve. The simulation results are in close agreement with the measurements for both the velocity direction and magnitude.

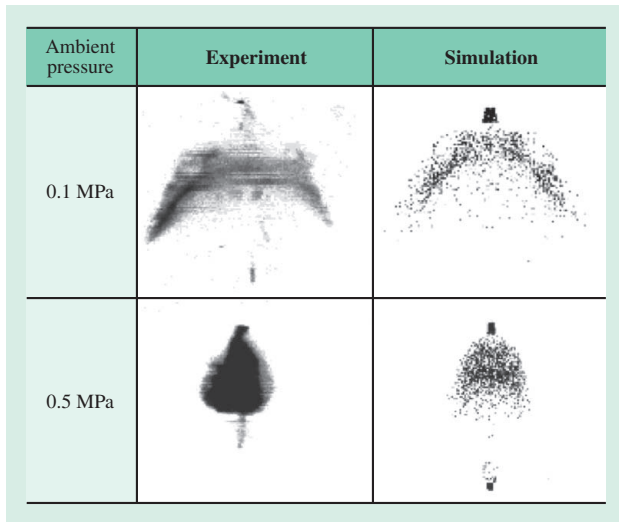


Fig. 7—Comparison of Experimental Measurements and Simulation Results for Fuel Spray. The figures show a central cross-section of the spray injected into still air using swirl-type injectors. The spray is injected from top of the figure toward the bottom. The figures on the left show a photograph of the actual spray captured using slit light, and those on the right show the simulation results. The results are shown for the cases when the air pressure is 0.1 MPa (atmospheric pressure) and 0.5 MPa (pressurized). Whereas the spray disperses outward at atmospheric pressure, the increased air resistance in the pressurized case makes the spray more consolidated. These changes in spray behavior at different pressures are reproduced by the simulation.

Fig. 7 shows a comparison of experimental measurements and simulation results for the fuel spray. The fuel injection valves used in the analysis are swirl-type fuel injectors that atomize the fuel by imparting a swirling motion to it, and which produce a hollow cone-shaped spray when the ambient pressure is 0.1 MPa. With an ambient pressure of 0.5 MPa, the spray becomes more consolidated due to a flow from the surroundings being drawn into the center of the swirling spray. These differences in spray shape associated with differences in ambient pressure were accurately reproduced by the simulation.

Verification of Combustion Simulations

Fig. 8 shows an example simulation of combustion and PM formation. It uses a contour diagram to show the simulation results over a horizontal cross-section of a direct injection gasoline engine cylinder. From the top, the diagrams show the flame propagation (burnup fraction distribution), equivalence ratio distribution, and PM particle density distribution respectively. The simulation models the ignition of the flame by the spark plug at the center of the cylinder

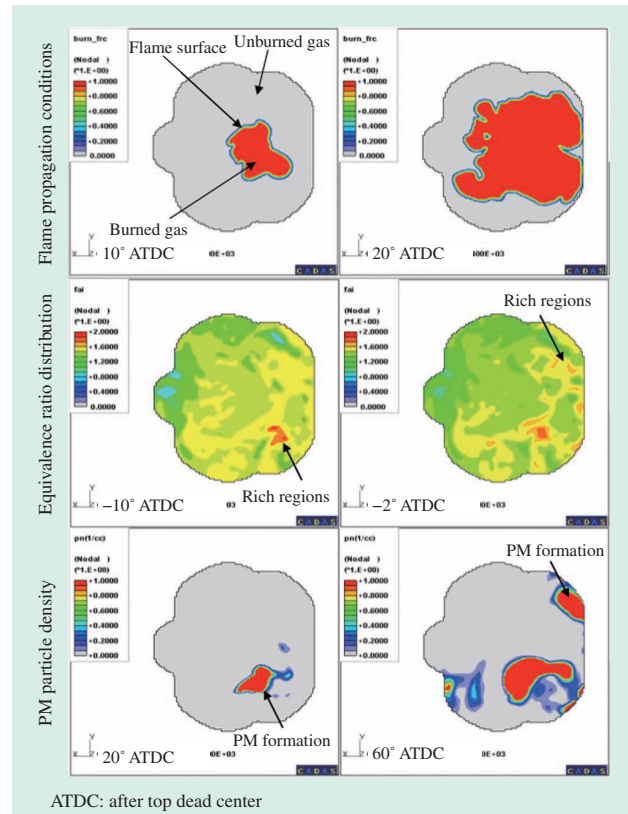


Fig. 8—Example Simulation of Combustion and PM Formation. These contour graphs represent a horizontal cross-section across the engine cylinder and show the results of simulating combustion and PM formation in a direct injection gasoline engine. The top graphs show the distribution of combustion gas, with the red regions representing burned gas and the grey regions representing unburned gas. The boundary between the two is the flame surface. The graphs in the middle show the distribution of the equivalence ratio (fuel concentration), with red representing fuel-rich regions. The bottom graphs show the density of PM particles, with red representing regions of high PM concentration. The graphs show how high concentrations of PM are formed in the fuel-rich regions in the cylinder.

and its propagation out to the cylinder walls. From the equivalence ratio distribution and PM particle density distribution, it can be seen that PM formation starts primarily from a fuel-rich area that forms at the exhaust side of the cylinder (right).

Fig. 9 shows a comparison of experimental measurements and simulation results for the time-evolution of pressure inside an engine cylinder. Fig. 10 shows a comparison of experimental measurements and simulation results for the number of PM particles emitted by the engine. These show good agreement between the experimental and simulation results for how the equivalence ratio changes the behavior of combustion pressure and the quantity of PM emissions.

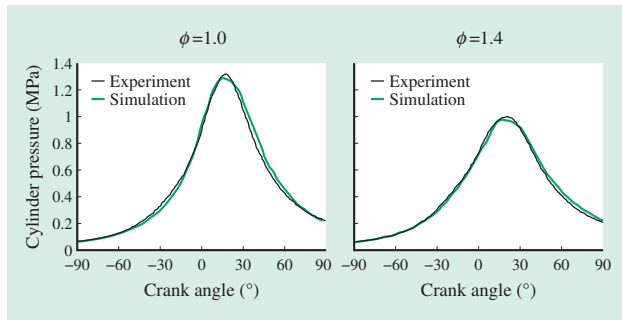


Fig. 9—Comparison of Time-evolution of Pressure Inside Engine Cylinder.

The graphs show a comparison of experimental measurements and simulation results for the time-evolution of pressure inside an engine cylinder. The horizontal axis represents the engine crank angle, with 0° representing the uppermost point of the piston's stroke (top dead center). The black lines are the experimental measurements and the green lines are the simulation results. The graphs on the left show the case when the mean equivalence ratio is 1 (stoichiometric mixture ratio) and those on the right show the case when the mean equivalence ratio is 1.4 (fuel-rich mixture). The combustion rate and cylinder pressure vary depending on the equivalence ratio. This variation is reproduced by the simulation.

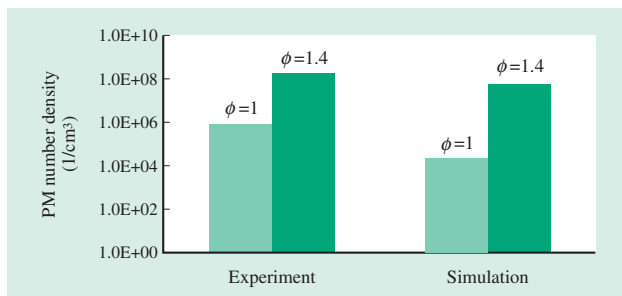


Fig. 10—Comparison of PM Number Density.

The graphs show experimental measurements and simulation results for the number density of PM emitted by the engine. The graph on the left shows the measurements and the graph on the right shows simulation results. ϕ is the mean equivalence ratio. The higher the mean equivalence ratio (the richer the mixture) is, the more PM concentration increases. This effect is reproduced by the simulation.

APPLICATION TO SPARK IGNITION ENGINES

Use for Reducing Unburned HCs

The use of exhaust heating to achieve early activation of the catalyst and promote the oxidation of unburned HCs are effective techniques for reducing emissions after a cold start-up. A good way to achieve exhaust heating is to delay combustion by making the spark timing later than normal. However, while the exhaust temperature is increased by a later spark timing, it has

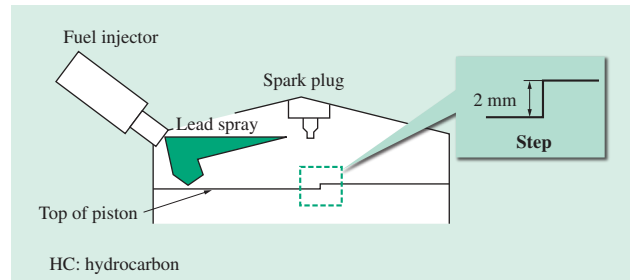


Fig. 11—Piston Shape and Spray Direction.

The diagrams show the engine piston shape and spray shape used by a combustion concept for reducing unburned HC. The concept involves locating a small step in the center of the piston's top surface (stepped crown) and using injectors that produce an asymmetrical spray.

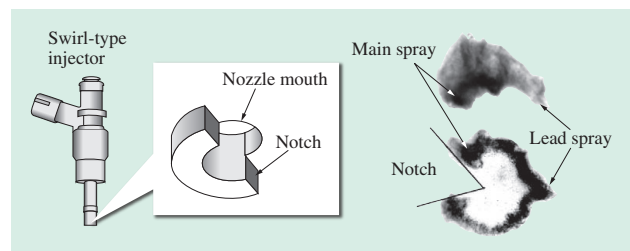


Fig. 12—Nozzle Shape and Spray Pattern.

The diagrams show the nozzle shape for producing an asymmetrical spray and the resulting spray pattern (obtained by observation). A notch in the tip of the nozzle of the swirl-type injector produces both a lead spray with high penetration force and a main spray with superior atomization.

the unfortunate side effect of increasing cyclic torque variation. To prevent this, it is necessary to improve the ignitability of the mixture to stabilize combustion, particularly at the early stage when the engine is most prone to cyclic variation. Accordingly, Hitachi has used a computer simulation to develop a combustion concept that reduces unburned HCs after a cold start-up. The following section describes an example⁽⁸⁾.

The combustion concept is based on using a piston with a stepped crown (see Fig. 11). This involves having a small step in the central part of the top surface (crown) of the piston. It also uses swirl-type fuel injectors that can produce an asymmetrical spray with respect to the spark plug and piston axes⁽⁹⁾ (see Fig. 12). These injectors have a step-shaped notch in their nozzles to generate an asymmetrical spray. Consisting of both a lead spray with high penetration force and a main spray with superior atomization, a feature of the spray is that the injection direction of the lead spray remains unchanged at high ambient pressures. The injectors are located so as to aim this directed lead spray at the area under the spark plug electrodes.

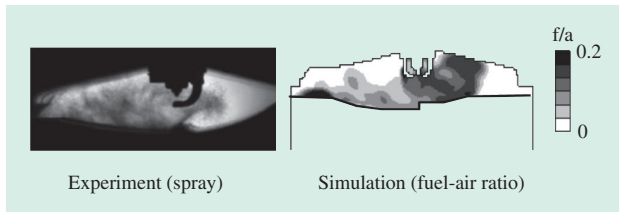


Fig. 13—Fuel Behavior in Engine Cylinder.
The figures show the behavior of fuel in the engine cylinder around the time of ignition when using the combustion concept for reducing unburned HC. The figure on the left shows the fuel spray distribution observed in a transparent engine and the figure on the right shows the fuel concentration (fuel-air ratio) distribution obtained by simulation. A flow from the center of the piston toward the spark plug concentrates the fuel around the spark plug.

When this piston-shaped spray is used to inject fuel during the latter part of the compression stroke, the rapid gas flow produced by the lead spray causes the pressure around the spark plug to drop. The flow resulting from the main spray, meanwhile, decelerates at the stepped crown of the piston and causes an increase in pressure. This pressure difference causes an upward flow from the stepped crown toward the spark plug, resulting in the fuel around the top of the piston being concentrated around the spark plug (see Fig. 13).

For most hydrocarbon fuels such as gasoline, flame propagation is improved by using a mixture that is slightly richer than the stoichiometric mixture ratio. Accordingly, the initial combustion can be stabilized by concentrating the fuel around the spark plug in this way, allowing a longer delay in ignition timing after a cold start-up. The benefits of simulation include, for example, its use to determine the optimal piston shape quickly.

Fig. 14 shows the results of a simulation of different piston shapes conducted to determine how the mixture concentration in the vicinity of the spark plug is influenced by small changes in the spray shape. The results show that piston B has a more robust mixture formation with less variability in mixture concentration.

Fig. 15 shows measurements of exhaust temperature and cumulative unburned HC emissions after a cold start-up. The exhaust temperature was measured at the part of the manifold where the exhaust pipes from each cylinder merge and the HC was measured at the tail pipe (after passing through the three-way catalyst). The measurements were conducted for pistons with and without a stepped crown. Because the more stable combustion for the pistons with a stepped crown allows the ignition timing to be

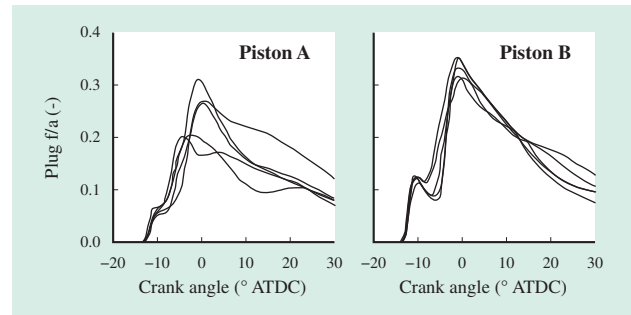


Fig. 14—Variation in Mixture Concentration around Spark Plug for Different Spray Shapes (Simulation Results).
The graphs show the results of simulating how small changes in the fuel spray shape affect the fuel concentration (fuel-air ratio) in the vicinity of the spark plug. Reducing variability helps achieve stable combustion. Simulations were used to design the optimal piston shape for producing a robust mixture.

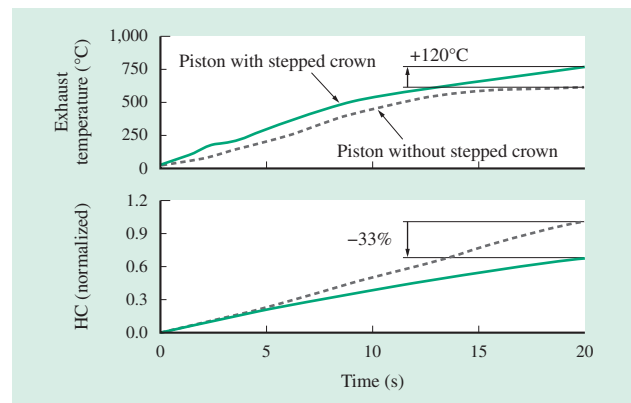


Fig. 15—Exhaust Temperature and Cumulative Unburned HC Emissions after a Cold Start-up (Measurements).
The graphs show measurements for the exhaust temperature and cumulative unburned HC emissions after a cold start-up. This demonstrates how the concept increases exhaust temperature and reduces unburned HCs.

delayed, the exhaust temperature is 120°C higher than for the other piston and the cumulative unburned HC emissions are 33% lower. It is believed that this reduction in unburned HCs is a result both to the greater oxidization of unburned HCs in the exhaust pipe due to the higher exhaust temperature and the earlier activation of the three-way catalyst. These verification results demonstrate that this combustion concept is an effective way of reducing unburned HCs after a cold start-up.

Use for Reducing PM

Fuel droplets that have adhered to the piston surface and cylinder walls are the main cause of PM in cold gasoline engines. Because fuel that has adhered to a surface is impeded from mixing with the air, the

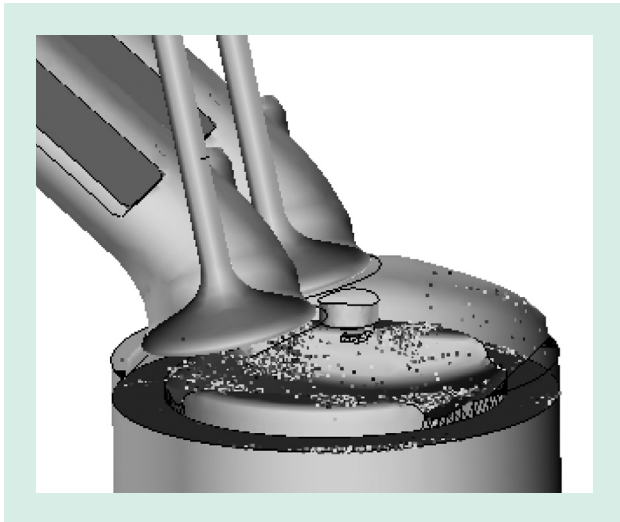


Fig. 16—Results of Simulating Adhesion of Droplets to Surfaces (without Split Injection).

The figure shows the results of simulating the adhesion of fuel droplets to surfaces in a direct injection gasoline engine. This adhesion is a cause of PM formation in cold engines.

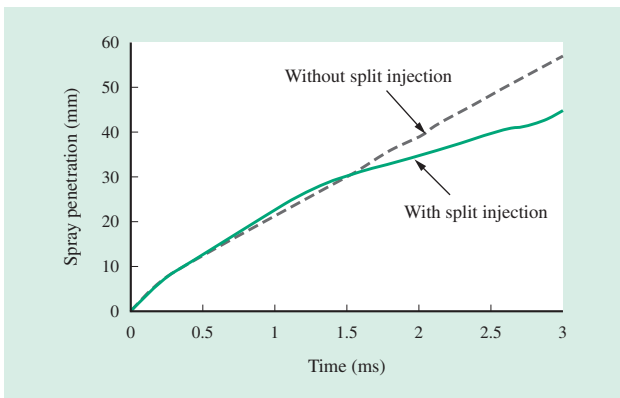


Fig. 17—Results of Simulating Spray Penetration. The graphs show the results of simulating the spray penetration (distance reached by leading edge of spray). Split injection reduces penetration because it increases the interference between spray and air.

phenomenon results in the formation of a localized region of fuel-rich mixture that is the source of PM. Fig. 16 shows the results of a simulation of fuel droplets adhering to surfaces in a direct injection gasoline engine.

Because a direct injection gasoline engine involves the injection at high speed of fuel droplets into the confined space inside the cylinder, the penetration force of the spray itself tends to cause droplets to adhere to surfaces. An effective way to reduce the penetration force of the spray is to repeat injection a number of times. Fig. 17 shows the results of a simulation demonstrating how use of this split

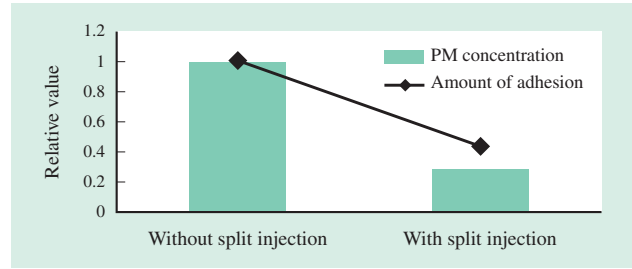


Fig. 18—Adhesion and PM Reduction Benefits of Split Injection (Simulation Results).

The graph shows the results of simulating the reduction in fuel adhesion and PM resulting from use of split injection. The shorter penetration when using split injection reduces PM by reducing the adhesion of fuel to surfaces.

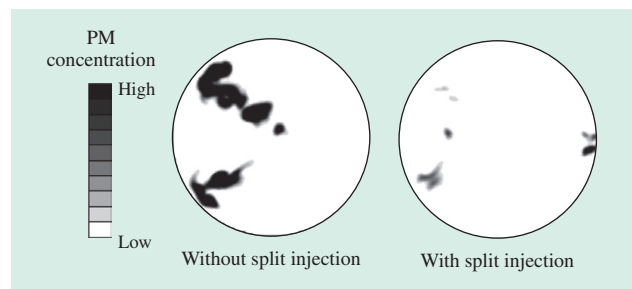


Fig. 19—Results of Simulating PM Concentration Distribution. The figures show the results of simulating the distribution of the PM concentration across a cross-section of an engine cylinder. Black represents high PM concentration. The results show that use of split injection shrinks the region of high PM concentration.

injection technique reduces the depth of spray penetration. Performing injection intermittently increases the interference between spray and air and increases the deceleration of droplets due to air resistance. By reducing the adhesion of fuel to cylinder walls, split injection significantly reduces the quantity of PM formed (see Fig. 18 and Fig. 19).

CONCLUSIONS

This article has described combustion simulation techniques used to aid engine system development.

The new techniques use simulations to estimate a series of physical phenomena that occur inside a cylinder as part of the engine cycle, including flow, fuel spray, mixture formation, and combustion. They also use detailed chemical reaction mechanisms as a basis for estimating the PM and other emissions that are formed during combustion.

These simulation techniques can be used for the efficient development of engine systems, which contain a large number of control parameters. The use

of simulations to view what is happening inside the cylinder is also likely to suggest ideas for innovative approaches to combustion control.

The complexity of what happens inside an engine means that numerous challenges remain in the field of simulations. Examples include combustion problems such as knocking or preignition, detailed ignition phenomena, flame quenching and heat transfer in the vicinity of surfaces, and cyclic variation. The more closely engine combustion is studied, the greater the demands that are likely to be placed on simulations. Hitachi intends to continue enhancing its simulation techniques to contribute to future engine system development.

REFERENCES

- (1) J.H. Ferziger et al., "Computational Methods for Fluid Dynamics," Springer-Verlag (1997).
- (2) A. D. Gosman et al., "Computer Analysis of Fuel-Air Mixing in Direct-Injection Engines," SAE Technical Paper No. 800091 (1980).
- (3) E. Ishii et al., "Simulation of Multi-Scale Free Surfaces within Gas-Liquid Flows Using Combined Particle and Grid Methods," *Thermal Science & Engineering* **14**, No. 3 (2006) in Japanese.
- (4) S. Inage et al., "A Proposal for a New Turbulent Combustion Model and Its Evaluation: 1st Report, Development of the Model," *Transactions of the Japan Society of Mechanical Engineers B* **61**, No. 586, 2290–2297 (1995) in Japanese.
- (5) Z. Wen et al., "Modeling Soot Formation in Turbulent Kerosene/air Jet Diffusion Flames," *Combustion and Flame* **135**, pp. 323–340 (2003).
- (6) D. Carbonell et al., "Implementation of two-equation soot flamelet models for laminar diffusion flames," *Combustion and Flame*, Vol. 156, pp. 621–632 (2009)
- (7) H. Kawazoe et al., "Numerical Prediction of Steady Intake Flow in Engine, 68th Annual Conference of The Japan Society of Mechanical Engineers **68**, Pt C, No. 500-9, pp. 268–270 (1990) in Japanese.
- (8) Y. Sukegawa et al., "Study of Reduction Method of Hydrocarbon Emission during Cold-start for Direct Injection Gasoline Engines," *Transactions of the Society of Automotive Engineers of Japan* **41**, No. 5, pp. 1037–1042 (2010) in Japanese.
- (9) M. Abe et al., "Fuel Spray Pattern Control Using L-Step Nozzle for Swirl-Type Injector," SAE Technical Paper, No. 2004-01-0540 (2004).

ABOUT THE AUTHORS



Yoshihiro Sukegawa

Green Mobility Research Department, Information and Control Systems Research Center, Hitachi Research Laboratory, Hitachi, Ltd. He is currently engaged in research and development of automotive engine combustion systems. Mr. Sukegawa is a member of the Society of Automotive Engineers International (SAE), Society of Automotive Engineers of Japan (JSAE), The Japan Society of Mechanical Engineers (JSME), and the Combustion Society of Japan.



Kazuhiro Oryoji

Green Mobility Research Department, Information and Control Systems Research Center, Hitachi Research Laboratory, Hitachi, Ltd. He is currently engaged in research and development of automotive engine combustion systems. Mr. Oryoji is a member of the JSAE and the Combustion Society of Japan.



Eiji Ishii, Dr. Eng.

Advanced Simulation Research Department, Mechanical Engineering Research Center, Hitachi Research Laboratory, Hitachi, Ltd. He is currently engaged in research and development of numerical simulation technologies for multiphase and multi-scale flow. Dr. Ishii is a member of the American Society of Mechanical Engineers (ASME), JSME, and The Japanese Society for Multiphase Flow.